Performance Analysis of Resin-infilled, Additive Manufacturing (3D printed), Polymer Structures, using Gyroid Pattern Infill

Asset Rakishev[1], Peter G. Gough[2], Craig E. Banks[2], Carl Diver[2]

[1] Abylkas Saginov Karaganda Technical University, Nursultan Nazarbayev ave. 56, 100027 Karaganda, Kazakhstan, a.rakishev@ktu.edu.kz

[2] Manchester Metropolitan University, Chester Street, M1 5GD, Manchester, United Kingdom, a.rakishev@ ktu.edu.kz, p.gough@mmu.ac.uk, c.banks@mmu.ac.uk, c.diver@mmu.ac.uk

Abstract: Additive manufacturing is rapidly expanding across various industrial sectors, due to its design flexibility and material efficiency. Among AM techniques, fused deposition modelling remains the most widespread for fabricating polymer components. The mechanical performance of printed parts largely depends on process parameters, particularly infill density. In this study, a novel approach is employed, by filling FDM-printed polylactic acid specimens, with epoxy resin to enhance the mechanical properties. Gyroid infill topology was selected, owing to its continuous and interconnected geometry, which allows complete resin penetration. Experimental investigations were conducted on specimens with 25%, 50%, and 100% infill densities, using two types of epoxy resin. Tensile, flexural, and compression tests were performed to evaluate the influence of resin infiltration. The results revealed that resin type significantly affects the mechanical responses. While solid PLA samples exhibited the highest tensile and compressive strengths, the epoxy-infilled composites demonstrated improved flexural performance and reduced printing time, indicating the potential of this approach for lightweight, time-efficient, manufacturing applications.

Keywords: Additive Manufacturing; FDM; Gyroid Infill; Epoxy Resin; Mechanical Properties

1 Introduction

One of the essential factors of global manufacture is the reduction of material costs, development time, and labor intensity. Additive manufacturing (AM), also known as 3D printing, is a group of promising technologies that address these criteria. A key advantage of AM is the ability to achieve previously unattainable component characteristics, namely complex spatial configurations, customized form and design, and improved performance properties when using advanced materials.

Additionally, AM is a cost-effective technology due to reduced use of materials and labor costs compared with traditional processing methods. Today, 3D printing is applied not only in prototyping and distributed manufacturing but also in a wide range of industries, including architecture, industrial design, engineering, medicine, and fashion.

AM comprises seven different processes [1]. Products can be fabricated in layers by extrusion, UV curing, lamination or material fusion. Extrusion-based processes are currently the most widespread in terms of the number of machines and users, mainly due to their low maintenance cost, ease of access, and simple workflow. Fused deposition modelling (FDM), also called fused filament fabrication (FFF), is a widely used extrusion-based technique. In this process, an object is built by depositing molten thermoplastic material, layer by layer, according to a pre-programmed toolpath.

3D printing process involves a number of parameters that influence the properties of printed parts. Setting these parameters allows changes in mechanical efficiency design and is highly favorable for reducing material consumption and time [2-5]. Currently, numerous researchers have conducted detailed studies and discussed the influence of different extrusion-based printing parameters on part quality. The variables most frequently considered in these studies are: infill density and pattern [2, 4-17], build orientation [3, 4, 9, 11, 16-21], layer height [4, 6, 11, 13, 17, 19, 21], print speed [4, 6, 13, 15, 17, 19], raster angle [3, 13, 21], number of shells [5] [11], extrusion temperature [4-5], nozzle diameter [5]. The results of the articles presented above support the conclusion that each indicated parameter, individually or in a set, can affect the mechanical properties of the print. In particular, many attempts were made to define the tensile strength of specimens under various print parameters.

One of the key parameters that positively affect the mechanical characteristics of printed part is the infill density [7] [10]. Many studies [6, 9, 17] confirm that infill percentage has the most significant weight compared to some process parameters. The volume of material increases with grater infill density, which positively affects its strength. On the other hand, a high infill ratio leads to higher energy consumption and build time [11] [15]. However, not only the infill density determines the mechanical properties of a 3D printed part. Authors in [18] examined the impact of three build orientations on mechanical and physical characteristics. The flat-oriented specimen showed relatively high mechanical performance, according to their results. Xu et al. [17] confirm that build direction plays a more critical role, especially in tensile and flexural strength. Horizontally built samples withstand tension and bending loads more effectively. In the same study, layer height also influenced compressive strength, although its effect was ambiguous. While high layer thickness was required for tensile performance, an intermediate value was preferable for compression and bending. A comparable effect was reported earlier by Sood et al. [21], where layer height was analyzed together with four other process

variables and their interactions. Based on compression test results, they suggested optimal values.

Another study conducted by Kumar et al. [13] determined the effect of print speed, raster angle, and two additional parameters on the mechanical properties of the FDM parts. In tensile, flexural and impact tests, it was found that feed rate is the primary factor affecting tensile strength. An increase in speed has a negative effect. Regarding raster angle, it also modifies tensile behavior. In terms of impact and flexural strength, raster angle is significant, with layers oriented at ±45° showing greater bending and impact resistance.

Apart from the parameters mentioned above, the mechanical behavior of FDM products is also influenced by extrusion temperature, nozzle diameter, and the number of shells. In their study, Le et al. [5] characterized the ultimate tensile strength under varied print settings such as the number of outer shells, nozzle diameter, extrusion temperature, and infill range. Experiments were carried out using PLA specimens, and the results indicated that an increase in the number of shells, nozzle diameter, and extrusion temperature enhanced tensile strength. A high deposition temperature ensured proper fusion between layers and reduced porosity in the specimens. Furthermore, Alafaghani et al. [4] reported that improvements in strength occur at specific temperature values.

Previous studies have demonstrated that the mechanical properties of FDM parts are affected by a range of process parameters. Infill density and pattern have been shown to play a decisive role, with higher infill levels improving strength but also increasing print time and material usage [6, 9, 10, 17]. Build orientation and layer height also influence performance: horizontally printed specimens often provide better tensile and flexural behavior, while the effect of layer thickness depends on the loading mode [17] [21]. Other parameters such as raster angle, number of shells, extrusion temperature, and nozzle diameter contribute to variations in tensile, flexural, and impact properties [5] [13]. These findings underline that no single parameter determines performance in isolation, and mechanical behavior is governed by a combination of process settings.

In recent years, alternative approaches to reinforce additively manufactured parts have been explored by filling lattice or cellular structures with soft or semi-rigid materials. For example, Széles et al. investigated a doubly re-entrant auxetic lattice structure modified with silicone filling for impact absorption applications. Under quasi-static compression, the filled structures dissipated more than twice the energy compared with unfilled counterparts, confirming the effectiveness of silicone as a filler material in enhancing damping and absorption capacity. [22]. Choudhry et al. proposed modified two-dimensional re-entrant auxetic lattice designs with additional vertical ligaments, which provided enhanced stiffness (up to +355%) and superior energy absorption (up to +165%) compared with conventional auxetic lattices of the same mass [23]. Black et al. investigated gel-filled prismatic lattices produced from PLA, PET-G, and ABS, showing that agar-filled specimens

significantly enhanced energy absorption (up to 46.1%) and displacement to failure (57.4%) compared with unfilled controls under quasi-static compression [24]. Other works applied functionally graded shell lattices as infill in an additively manufactured bicycle crank arm and demonstrated that spatial variation of lattice density can reduce weight while significantly increasing stiffness-to-mass ratio (by over 100%), thereby improving structural performance [25]. In the context of 3D printing, recent reviews [26] [27] have examined biomimetic lattice structures as well as cellular and lattice-based metamaterials produced by fused filament fabrication. These studies discussed classification, mechanical performance, optimization strategies, and manufacturing challenges. Both emphasize that infill architectures behave analogously to lattice metamaterials, with mechanical response strongly governed by their topology and relative density. These studies suggest that infill patterns behave similarly to lattice metamaterials, and strategies developed for lattice filling may be relevant to improve mechanical behavior of FDM parts.

Nonetheless, few studies have specifically considered epoxy resin infilling of PLA printed parts, particularly using gyroid or TPMS-based infill, to enhance mechanical properties. This gap motivates the current work to explore resin-infilled gyroid PLA structures and assess their mechanical performance under tensile, flexural, and compression loading. Considering the factors mentioned earlier, besides processing parameters, the ability of a print to resist external forces is largely determined by the material. By adding reinforcing elements to thermoplastic filaments, it is possible to increase strength. Krajangsawasdi et al. [28] categorized types of fiber reinforcements in FDM and showed that the mechanical performance of reinforced materials was significantly improved. However, very few studies have assessed the effect of epoxy resin as an infill for FDM technology. Epoxy resins have a wide range of applications, provide strong adhesion, and can achieve favorable mechanical properties [29].

In the study by Sathishkumar et al. [30], acrylonitrile butadiene styrene (ABS) parts were infilled with epoxy and polyester resins. Compression tests showed that specimens infilled with epoxy resin exhibited substantial improvements in strength compared with other samples; the resin also demonstrated good adhesion to the base polymer. Nevertheless, only a limited number of studies address the mechanical behavior of FDM parts with epoxy infill. This research was therefore undertaken to fill this gap.

In the current work, a novel approach was developed by filling resin into additively manufactured elements. To ensure complete filling of internal cavities with epoxy, a gyroid infill pattern was selected. A gyroid is a continuous, infinitely repeating three-dimensional structure. This nature-inspired pattern offers several advantages, including favorable mechanical characteristics combined with lightweight construction [31]. Its principal feature is that all channels are interconnected, which enables unhindered resin infill. The present study employs gyroid pattern infill to analyze the mechanical performance of epoxy resin-infilled, 3D-printed polylactic

acid (PLA) structures. To evaluate the quality of resin infill within the internal channels and to conduct fractographic analysis, an S1000 industrial stereo microscope was used.

2 Materials and Methods

In this study, three types of specimens were prepared for mechanical testing: tensile, flexural, and compression, as illustrated in Figure 1. All specimens were manufactured from PLA filament, while additional series were produced with epoxy resin infill. The investigated parameters were infill density (25%, 50%, and 100%) and resin type (Craft Resin and EL2 Resin). Infilled specimens were fabricated by filling the internal structure of PLA parts with epoxy; specifically, the specimens with 25% and 50% infill density were selected for resin filling. Other printing parameters were kept constant, as summarized in Table 2. The following subsections provide details on the materials, printing conditions, and testing procedures.

2.1 Materials, Equipment and Specimen Preparation

In this study, the mechanical strength of parts produced by FDM technology and reinforced with epoxy resin is examined. A polylactic acid (PLA) filament manufactured by Filamentive Ltd. (UK), 2.85 mm in diameter and white in color, was selected as the printing material. PLA is one of the most widely used and versatile polymers in fused filament fabrication, with broad application among both industrial and individual users. Preparation of epoxy resin requires the addition of a hardener. This work utilized two types of epoxies: Craft Resin (Craft Resin Ltd., UK) and EL2 epoxy laminating resin (Easy Composites Ltd., UK). The corresponding mixture ratios are presented in Table 1. Adding the hardener in specific proportions initiates a chemical reaction that leads to solidification of the resin after a defined curing period. The prepared epoxy was manually injected into the printed specimens at room temperature.

Table 1
Mix ratio for epoxy resin

Epoxy Resin	Resin/hardener ratio	Curing time (hrs)
Craft Resin	1/1	24
EL2 epoxy laminating resin	100/30	24

PLA specimens were fabricated using an Ultimaker S5 3D printer operated with Cura slicing software, which generated the G-code and controlled the process parameters. All models were designed in Autodesk Fusion and exported in STL format. Figure 1 presents the general dimensions of the prepared specimens.

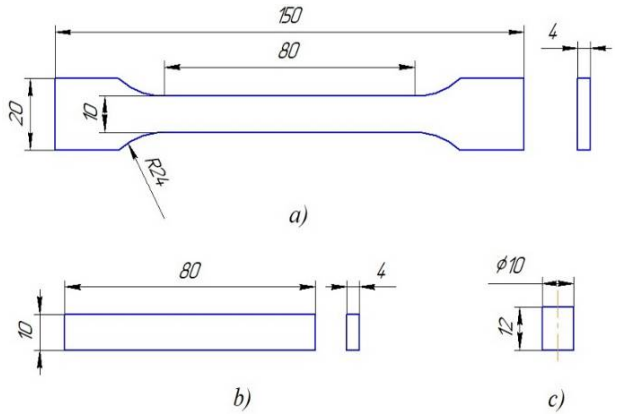

Figure 1
Dimensions of standard specimens (a) Tensile specimen (b) Flexural specimen (c) Compression specimen

2.2 Process Parameters

As concluded from previous studies, process parameters play a crucial role in determining the quality of printed components. However, no single article provides an exhaustive set of parameters to achieve optimal results across different mechanical tests. In this study, several parameters were kept constant for all specimens, taking into account equipment manufacturer recommendations and prior experience with print settings. The values presented in Table 2 were selected to enhance static strength while reducing printing time.

Table 2
Set of print parameters

Parameter	**Values/Range**	**Notes**
Filament material	PLA	Constant for all specimens
Build orientation	Flat	Fixed
Layer height	0.2 mm	Fixed
Print speed	60 mm/s	Fixed
Raster angle	+45°/-45°	Fixed
Number of shells:		
- walls	2	Fixed
- top/bottom layers	4	Fixed
Infill pattern	Gyroid	Fixed
Extrusion temperature	208°C	Fixed

Build plate temperature	60°C	Fixed
Nozzle diameter	0.8 mm	Fixed
Cooling fan speed	100%	Fixed
Infill density	25%, 50%, 100%	Varied
Resin type	Craft Resin; EL2 Resin	Varied (for infilled specimens)

The parameters listed in Table 2 were fixed to ensure consistency and reliability of the experimental procedure. The build orientation was kept flat, as this configuration is widely reported to provide higher tensile and flexural strength compared with vertical or inclined orientations [17] [21]. A layer height of 0.2 mm was selected as a compromise between surface quality, mechanical performance, and build time, with both lower and higher values shown in previous studies to be less optimal for certain loading conditions [21]. The raster angle of ±45° was adopted because this orientation has been found to increase impact resistance and flexural behavior compared with the 0°/90° rasters [13]. The number of shells was fixed at two for the walls and four for the top and bottom layers to guarantee structural integrity and avoid premature surface cracking [5]. Nozzle diameter was set to 0.8 mm, which improves deposition stability and reduces print time without compromising bonding between layers. The extrusion temperature of 208 °C was selected based on the recommended range for PLA, ensuring proper melting and interlayer adhesion while avoiding polymer degradation [4]. The build plate temperature was maintained at 60 °C to prevent warping and to improve first-layer adhesion, which is particularly important in larger specimens. Cooling fan speed was kept at 100% in order to achieve rapid solidification of the deposited material and stable geometry. Finally, the gyroid infill pattern was chosen because its interconnected channels allow uniform epoxy infill, making it particularly suitable for this study. By fixing these parameters, only infill density and resin type were varied, thereby isolating their effects on mechanical behavior.

For comparative analysis, three infill densities were selected: 25%, 50%, and 100%. Values below 25% do not provide a distinct or stable gyroid topology, which may prevent resin from fully penetrating the internal structure of the specimen. At densities above 50%, the gaps between adjacent structures become minimal, reducing the effectiveness of resin infill.

2.3 Experimental Set-up

This study involved three types of mechanical tests to evaluate the performance of resin-infilled printed parts: tensile, flexural, and compression. Two types of epoxy resin were used for a comprehensive analysis, both infilled into specimens with 25% infill density. In addition, pure PLA specimens with 25%, 50%, and 100% infill were also tested. A total of 75 tensile specimens were fabricated. For tensile testing, Type I specimens were prepared in accordance with ISO 527-2 (Type 1A) [32].

Flexural tests followed ISO 178 [33], while compression tests were conducted according to ISO 604 [34].

The uniaxial tensile test is one of the most commonly applied methods in mechanical characterization of materials. It determines strength and deformation behavior under tensile loading. Specimens were subjected to tensile testing at 1 mm/min until the modulus point, after which the test continued at 50 mm/min. A 100sz axial extensometer with a 50mm gauge length was used for strain measurements. Data were processed with the QMat software package, and all stress values were calculated based on the actual specimen dimensions.

The three-point bending test was conducted to evaluate flexural behavior. This method is widely applied for determining mechanical characteristics of brittle and polymeric materials. Data were collected using Horizon software. The support span was set to 64 mm, with loading applied at the midpoint over a 12 mm distance.

All tensile and three-point bending tests were conducted on a universal testing machine Hounsfield H10Ks (Tinius Hounsfield Test Equipment, UK) with a maximum load capacity of 10 kN at room temperature. Compression tests were performed using a Tinius Olsen 50ST (Tinius Olsen Ltd., UK) equipped with a 100 kN load cell. The tests were performed at a constant speed of 5mm/min at room temperature. Specimens were loaded over a 5 mm length, and average values from all measurements were taken as the final results.

2.4 Specimen Preparation and Resin Infilling

To ensure clarity on the resin filling procedure, specimens with 25% and 50% infill densities were selected for infiltration. The gyroid infill topology was chosen because its fully interconnected channels enable unhindered resin flow throughout the internal volume. Figure 2 shows the cross-section of three tensile specimens with 25% gyroid infill, as generated in the slicing software. Epoxy resin was injected manually using a syringe inserted into the inlet opening at one end of each specimen (Figure 3a). After filling, the samples were left at room temperature for curing. Figure 3b shows the infilled specimens after curing, where the inlet openings used for filling are clearly visible.

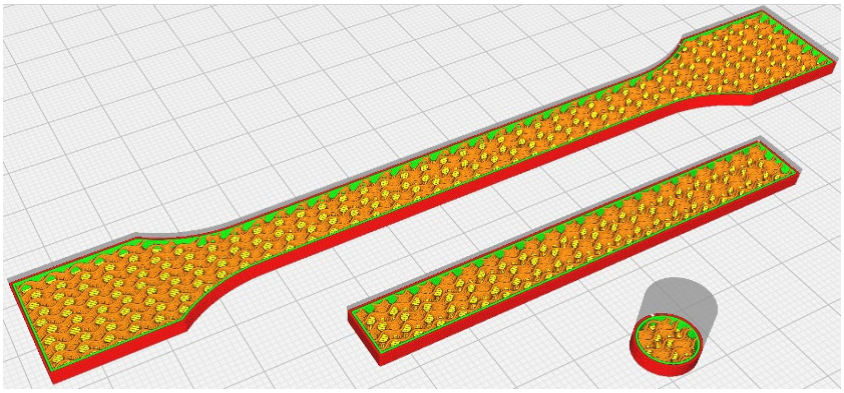

Figure 2
Cross-section view of tensile specimens with 25% gyroid infill generated in the slicing software Cura

To verify the quality of infiltration, the specimens were cut, and cross-sections were examined (Figure 3c). The cured epoxy resin, with a slightly yellowish tint, can be seen occupying all internal gyroid channels, indicating complete penetration and minimal void formation.

a)

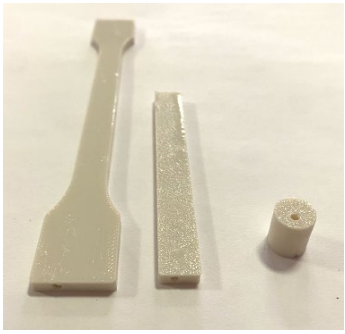

b)

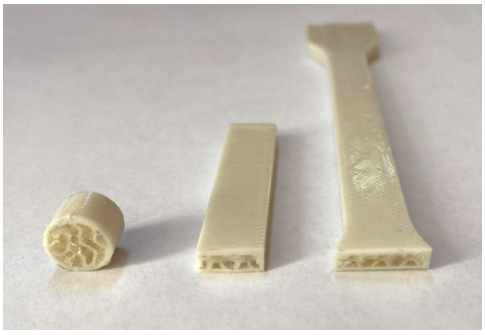

c)

Figure 3
Stages of the resin infiltration process for FDM-printed specimens with gyroid infill. (a) Manual resin injection into the printed specimen using a syringe. (b) Specimens after resin curing, showing inlet openings used for filling. (c) Cross-sectional view of infilled specimens, where the cured epoxy resin (light yellow) fully occupies the internal gyroid channels

3 Results and Discussion

3.1 Tensile Test

All specimen types were subjected to tensile, flexural, and compression tests. Figure 4 presents the force–displacement diagram obtained from the tensile tests. After data processing, the following mechanical properties were determined: strain, ultimate tensile strength (UTS), and elastic modulus (Young's modulus). Their values are summarized in Table 3.

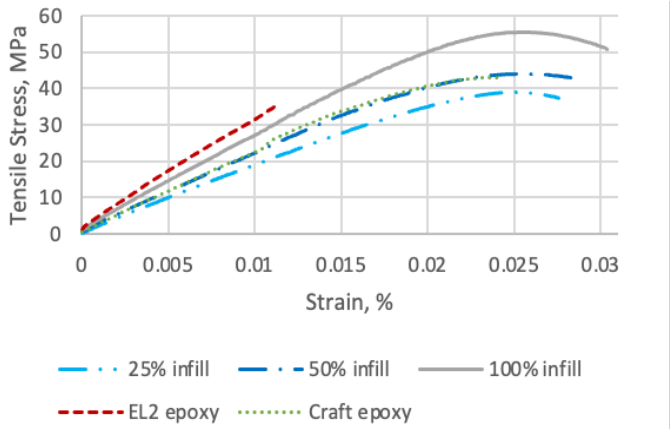

Figure 4
Tensile test graphs for all examined specimens

Table 3
Results of tensile test

Specimen Type	Tensile E-modulus (MPa)	Stress (MPa)	Strain (%)
with 25% infill	2059	39.2	2.56
with 50% infill	2303	42.61	2.7
with 100% infill	2964	56.2	3.184
Epoxy EL2	3011	34.7	1.16
Epoxy Craft	2183	42.11	2.38

As shown in Table 3, tensile strength increased gradually with higher infill density, from 39.2MPa at 25% to 56.2MPa for fully solid specimens. When comparing pure PLA with epoxy-infilled PLA, the effect of resin was less pronounced. Specimens with Craft resin showed only a modest increase of 2.9MPa, reaching values similar to those of PLA with 50% infill. In contrast, EL2 resin reduced tensile strength by approximately 11%, which may be attributed to internal voids and the brittle nature of the material, as discussed later.

The stress–strain curves can generally be divided into two regions frequently reported in the literature: an initial linear region corresponding to elastic deformation, followed by a nonlinear region where plastic deformation occurs, accompanied by strain hardening and necking. Resin-infilled specimens exhibited reduced deformation and a more brittle response, particularly for EL2 epoxy, which fractured without undergoing significant plastic deformation (Figure 4). In contrast, pure PLA showed a pronounced necking zone that expanded with increasing infill density. As illustrated in Figure 4, the elongation region became more evident after reaching maximum stress.

With respect to stiffness, the results followed a trend similar to tensile strength, except for EL2 epoxy, which exhibited an elastic modulus close to that of solid PLA due to its brittle behavior. On average, the elastic modulus of EL2 specimens was 47MPa higher than that of pure PLA.

3.2 Flexural Test

The three-point bending test results are presented in Figure 5. The curves demonstrate clear differences between pure PLA and resin-infilled specimens. Compared with the tensile test, flexural testing is more complex because the upper layers of a specimen are subjected to compression while the lower layers experience tension. This dual loading condition may explain the observed differences in behaviour between flexural and tensile specimens.

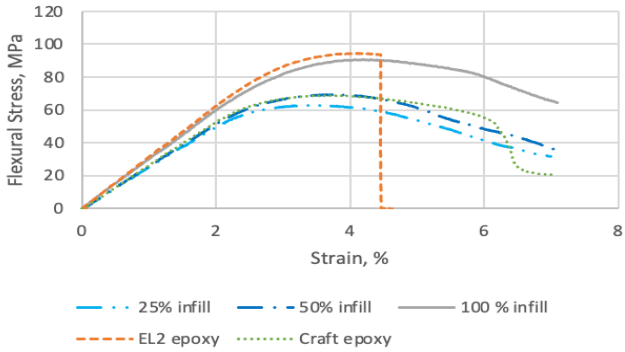

Figure 5
Flexural test graphs for all examined specimens

Overall, the results indicate that increasing infill density progressively enhanced flexural strength, as additional material improved resistance to bending. This effect is clearly visible in Figure 6, which compares the mechanical properties of all five specimen types. The use of epoxy resin did not produce a consistent trend. Notably, EL2 epoxy achieved the highest flexural stress of 93.91MPa, exceeding that of solid PLA, while Craft epoxy reached 68.78MPa, slightly lower than PLA with 50%

infill. In terms of flexural stiffness, however, Craft epoxy exhibited values higher than those of the 50% infilled specimens (Figure 6a). Flexural elastic modulus values generally followed the same trend as stress.

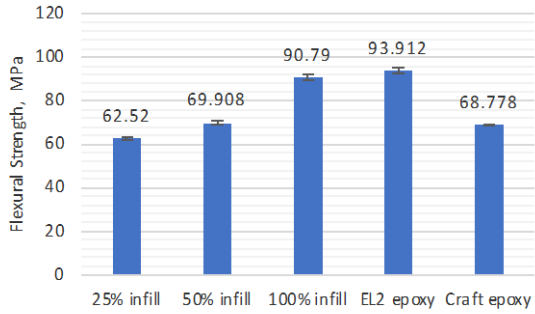

(a)

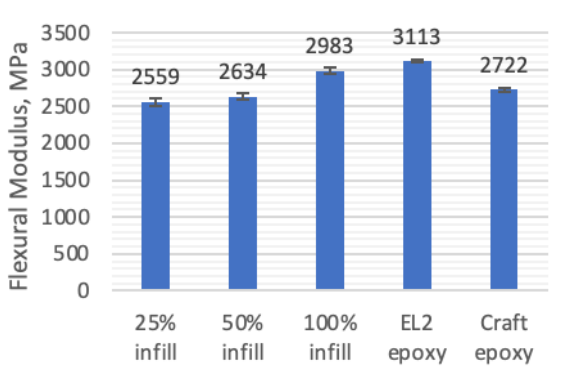

(b)

Figure 6

Comparison of average flexural properties for specimens: (a) Flexural stress (b) Elastic modulus

All specimens exhibited ductile behavior during the three-point bending test, with the exception of those containing EL2 epoxy. As shown in Figure 5, the EL2 curve terminates abruptly after reaching maximum stress, indicating brittle failure consistent with observations from the tensile test. Representative fractured specimens are presented in Figure 7. It can be seen that ductile specimens sustained only minor damage, typically limited to surface cracks in regions under tensile loading, whereas EL2 epoxy specimens failed in a brittle manner.

Figure 7
Examples of test pieces subjected to bending stress

3.3 Compression Test

The compression test results are shown in Figure 8. In general, all specimens exhibited similar behaviour characterised by two distinct regions: an initial linear region corresponding to elastic deformation, followed by a nonlinear region after the yield point. Once the yield point was exceeded, the load began to decrease as specimens started to barrel. With increasing strain, the specimens progressively lost their shape, compacted, and eventually fractured.

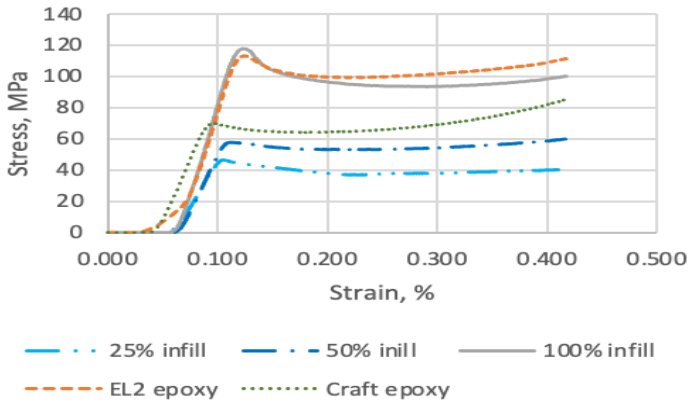

Figure 8
Compression test graphs for all examined specimens

The compressive load values ranged from 3632.6 to 9231.1 N, as summarized in Figure 9. Among all specimens, solid PLA demonstrated the highest resistance to compressive loading. EL2 epoxy specimens exhibited strength values close to those of fully dense PLA, while Craft epoxy specimens showed lower resistance. Considering that 25% infill PLA specimens were selected for resin reinforcement, compressive strength increased by approximately 1.5 times with Craft resin and by about 2.5 times with EL2 resin.

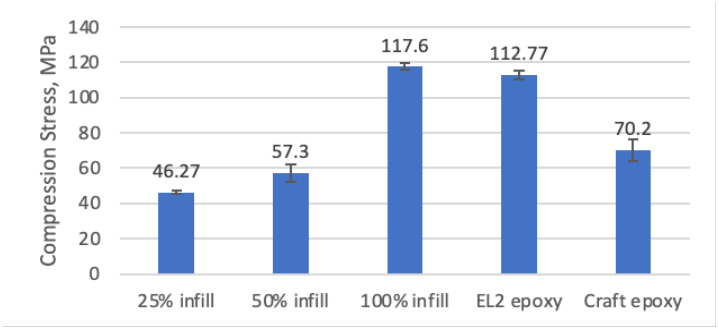

Figure 9
Comparison of average compression stress magnitudes

3.4 Fractographic Analysis

Fractographic analysis was carried out using an industrial stereo microscope to examine failure mechanisms in epoxy-infilled specimens. The images in Figure 10 reveal internal defects in the form of porosity and air gaps within the infilled regions. In Figure 10b, gaps between rasters forming the specimen wall are clearly visible. Epoxy resin also showed characteristic porosity after curing. Such internal defects act as stress concentrators and can reduce mechanical performance, which helps explain the differences observed between tensile and flexural tests. In tensile loading, stresses are distributed across the entire specimen, and failure typically initiates in regions with defect concentration. In flexural loading, the outer fibres bear the highest stresses; thus, the absence of external defects contributes to better resistance.

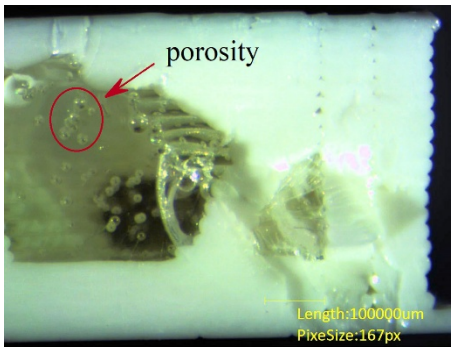

(a)

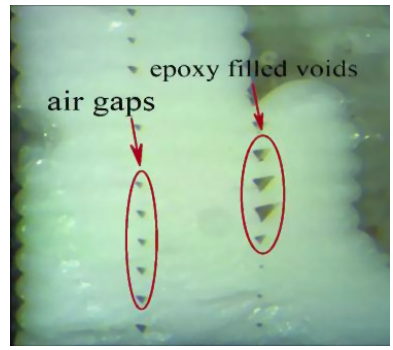

(b)

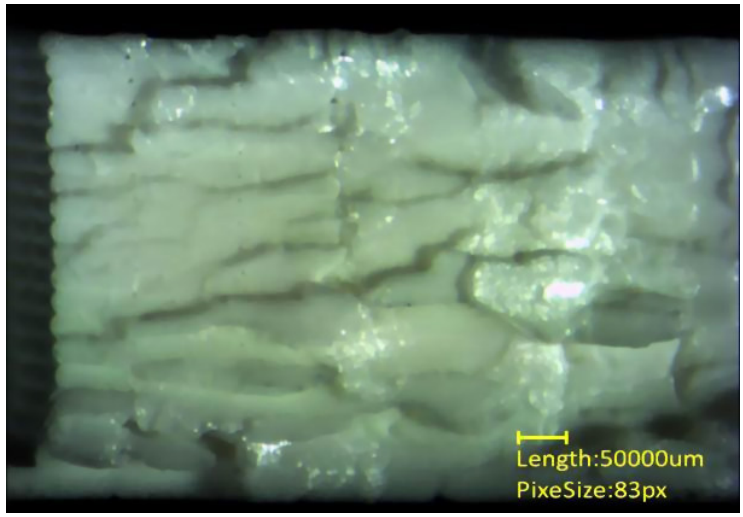

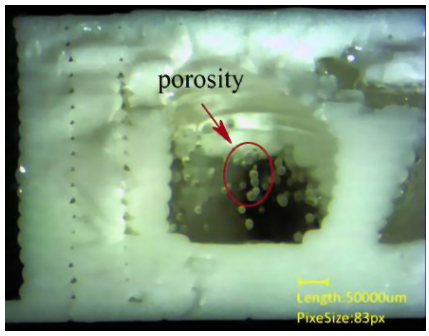

(c)

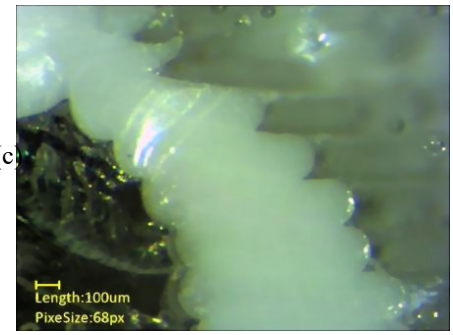

(d) (e)

Figure 10
Stereo microscope images of the fracture surfaces of (a)-(c) tensile specimens and (d)-(e) flexural specimens

Comparing the tensile fracture surfaces of resin-infilled and pure PLA specimens in Figures 8a and 8c, a relatively smooth surface can be observed for the EL2 epoxy specimen (Figure 10a), which indicates brittle behaviour. One of the features of the infilled resin is its strong bonding with the printed material. As shown in Figures 10b and 10e, the epoxy adhered well to both the infill pattern and the shell in the interface region without noticeable voids. A closer view of Figure 10b also reveals that the gaps between the infill pattern and walls were filled. These features contribute to the overall mechanical performance and enhance specimen stiffness.

The presence of air gaps and porosity in the specimens significantly affects mechanical strength [35]. During the fractographic analysis, small air voids were observed within the cured resin. To evaluate the possibility of minimizing such defects, an additional trial using a vacuum chamber was carried out after the main experiments. The results, shown in Figure 11, demonstrate a noticeable reduction in the number of voids within the resin body compared with the previously examined samples. This supplementary step was performed solely to verify the potential of vacuum treatment and was not included in the mechanical testing series.

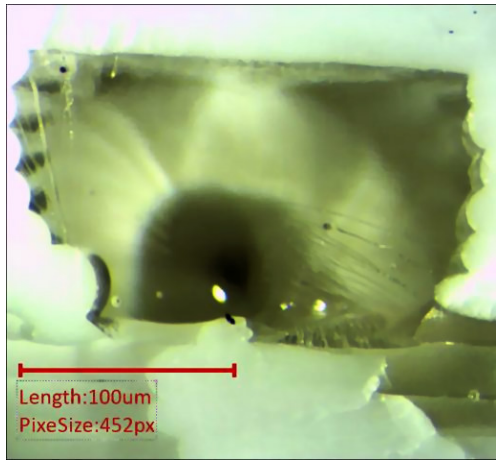

Figure 11
Images of the cross-sectional area of the specimen with EL2 epoxy after the vacuum chamber

In general, the results confirm that epoxy resin is a significant factor influencing the performance of FDM-printed parts. The study also revealed brittle behaviour combined with high stiffness in one type of epoxy-infilled specimen. An additional advantage of resin infill is the optimisation of printing time. Figure 12 summarises the outcomes of the three tests alongside the printing time required for a single specimen. The graph shows that the difference in printing time between 25% and 100% infill exceeds 50%. Reduced printing time, in turn, optimises the use of printer resources. With respect to mechanical strength, epoxy-infilled parts generally demonstrated comparable results. Specimens with EL2 resin exhibited

values close to the maximum, except in tensile stress. It can therefore be concluded that when mechanical properties are not the primary consideration and printing time is a more critical factor, epoxy resin infill can be a viable approach for FDM-printed parts.

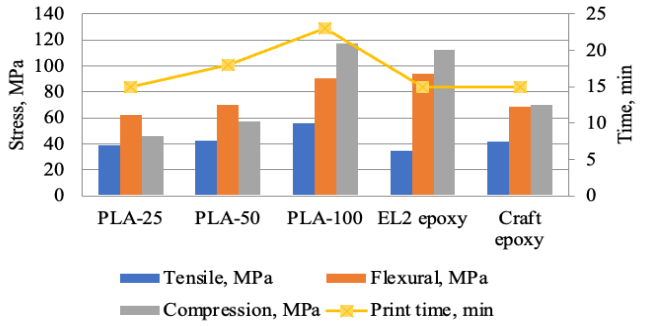

Figure 12
Comparisons of the tensile, flexural and compressive stresses with the print time

Conclusions

In consideration of the mechanical properties, the present study analyzed the performance of resin-infilled, 3D-printed PLA structures manufactured via FDM. This experimental work also addresses the lack of literature data concerning the mechanical behavior of epoxy-infilled polymer specimens. Tensile, flexural, and compression tests were conducted on samples with 25%, 50% and 100% infill densities, as well as on specimens filled with two types of epoxy resin (industrial and craft). Based on the results, the following conclusions are noted:

- The experiments demonstrate that increasing the infill density of PLA specimens, enhance their ability to withstand loading. In the case of epoxy-infilled samples, mechanical properties depend on the resin type and loading mode. EL2 epoxy notably increased the tensile modulus, thereby improving stiffness, although these specimens also exhibited low tensile strength and brittle behavior.
- EL2 epoxy-infilled specimens show the highest flexural strength, while compressive performance was comparable to that of solid PLA.
- Specimens with Craft epoxy displayed tensile, flexural and compressive behavior similar to PLA specimens, with 50% infill density.
- The shortest printing time was recorded for 25% infill specimens, which were subsequently used for resin infill. This novel approach thus offers a balance between reduced printing time and adequate mechanical performance for specific applications.

- The application of a vacuum chamber, reduced porosity-related defects observed in epoxy-infilled specimens during microscopic analysis, highlighting potential for further investigations of PLA/epoxy composites.

Acknowledgement

The authors gratefully acknowledge the support of JSC Center for International Programs through the Bolashaq program.

References

[1] ISO/ASTM52900 Additive Manufacturing – General Principles – Terminology. West Conshohocken, PA: ASTM International; 2015, https://www.astm.org/Standards/ISOASTM52900.htm

[2] S. Dev, R. Srivastava, Effect of infill parameters on material sustainability and mechanical properties in fused deposition modelling process: a case study, Progress in Additive Manufacturing (2021) 6:631-642, https://doi.org/10.1007/s40964-021-00184-4

[3] I. Durgun, R. Ertan, Experimental investigation of FDM process for improvement of mechanical properties and production cost, Rapid Prototyping Journal, 20/3 (2014) 228-235, doi 10.1108/RPJ-10-2012-0091

[4] A. Alafaghani, A. Qattawia, B. Alrawi, A. Guzman, Experimental Optimisation of Fused Deposition Modelling Processing Parameters: a Design-for-Manufacturing Approach, Procedia Manufacturing 10 (2017) 791-803, doi: 10.1016/j.promfg.2017.07.079

[5] L. Le, M.A. Rabsatt, H. Eisazadeh, M. Torabizadeh, Reducing print time while minimising loss in mechanical properties in consumer FDM parts, International Journal of Lightweight Materials and Manufacture 5 (2022) 197-212, https://doi.org/10.1016/j.ijlmm.2022.01.003

[6] A. Farazin, M. Mohammadimehr, Effect of different parameters on the tensile properties of printed Polylactic acid samples by FDM: experimental design tested with MDs simulation, The International Journal of Advanced Manufacturing Technology (2022) 118:103-118, https://doi.org/10.1007/s00170-021-07330-w

[7] M. Othmani, K. Zarbane, A. Chouaf, Effect of infill and density pattern on the mechanical behaviour of ABS parts manufactured by FDM using Taguchi and ANOVA approach, Archives of Materials Science and Engineering (2021) 111 (2), 66-77, DOI: 10.5604/01.3001.0015.5806

[8] J. Dobos, M. M. Hanon, I. Oldal, Effect of infill density and pattern on the specific load capacity of FDM 3D-printed PLA multi-layer sandwich, J Polym Eng (2022) 42(2): 118-128, https://doi.org/10.1515/polyeng-2021-0223

[9] R. Umapathi, J. H. Lim, Effect of Infill Pattern and Lattice Structure on the Mechanical Properties of 3D Printed Metal Polylactide Filament, 15th

International Engineering and Computing Research Conference (EURECA 2021) Journal of Physics: Conference Series 2120 (2021) 012019, doi:10.1088/1742-6596/2120/1/012019

[10] E. Cuan-Urquizo, A. Álvarez-Trejo, A. R. Gil, V. Tejada-Ortigoza, C. Camposeco-Negrete, E. Uribe-Lam, C. D. Treviño-Quintanilla, Effective Stiffness of Fused Deposition Modeling Infill Lattice Patterns Made of PLA-Wood Material, Polymers (2022) 14, 337, https://doi.org/10.3390/polym14020337

[11] C. A. Griffiths, J. Howarthb, G. de-Almeida Rowbotham, A. Rees, Effect of build parameters on processing efficiency and material performance in fused deposition modelling, Procedia CIRP 49 (2016) 28-32, DOI: 10.1016/j.procir.2015.07.024

[12] S. K. Selvamani, K. Rajan, M. Samykano, R. R. Kumar, K. Kadirgama, R. V. Mohan, Investigation of tensile properties of PLA-brass composite using FDM, Prog. Addit. Manuf. (2022) https://doi.org/10.1007/s40964-021-00255-6

[13] K. R. Kumar, V. Mohanavel, K. Kiran, Mechanical Properties and Characterization of Polylactic Acid/Carbon Fiber Composite Fabricated by Fused Deposition Modeling, J. of Materi Eng and Perform 31, 4877-4886 (2022) https://doi.org/10.1007/s11665-021-06566-7

[14] X. Zhou, Sh.-J. Hsieh, C.-Ch. Ting Modelling and estimation of tensile behaviour of polylactic acid parts manufactured by fused deposition modelling using finite element analysis and knowledge-based library, Virtual and Physical Prototyping, (2018) 13:3, 177-190, DOI: 10.1080/17452759.2018.1442681

[15] Ch. Abeykoon, P. Sri-Amphorn, A. Fernando, Optimisation of fused deposition modeling parameters for improved PLA and ABS 3D printed structures, International Journal of Lightweight Materials and Manufacture 3 (2020) 284-297, https://doi.org/10.1016/j.ijlmm.2020.03.003

[16] S. Tandon, R. Kacker, K. G. Sudhakar, Quantitative strength analysis for 3D-printed specimens in a Tri-Hexagon pattern, Proc IMechE Part C: J Mechanical Engineering Science 2021, Vol. 235(24) 7685-7698, DOI: 10.1177/09544062211021120

[17] J. Xu, F. Xu, G. Gao, The Effect of 3D Printing Process Parameters on the Mechanical Properties of PLA Parts, Journal of Physics: Conference Series, 2133 (2021) 012026, doi:10.1088/1742-6596/2133/1/012028

[18] Giulia Morettini, M, Palmieri, L. Capponi, L. Landi, Comprehensive characterisation of mechanical and physical properties of PLA structures printed by FFF-3D-printing process in different directions, Prog Addit Manuf (2022) https://doi.org/10.1007/s40964-022-00285-8

[19] J. M. Chacón, M. A. Caminero, E. García-Plaza, P. J. Núñez, Additive manufacturing of PLA structures using fused deposition modelling: Effect of process parameters on mechanical properties and their optimal selection, Materials and Design 124 (2017) 143-157, http://dx.doi.org/10.1016/j.matdes.2017.03.065

[20] T. Koziora, C. Kundera, Evaluation of the influence of parameters of FDM technology on the selected mechanical properties of models, Procedia Engineering 192 (2017) 463-468, DOI: 10.1016/j.proeng.2017.06.080

[21] A. K. Sood, R. K. Ohdar, S. S. Mahapatra, Experimental investigation and empirical modelling of FDM process for compressive strength improvement, Journal of Advanced Research (2012) 3, 81-90, doi:10.1016/j.jare.2011.05.001

[22] L. Széles, R. Horváth, L. Cveticanin, Research on auxetic lattice structure for impact absorption in machines and mechanisms, Mathematics, 2024, 12(13), 1983, https://doi.org/10.3390/math12131983

[23] N. K. Choudhry, B. Panda, S. Kumar, "Enhanced energy absorption performance of 3D printed 2D auxetic lattices," Thin-Walled Structures, 2023, 186, 110650, https://doi.org/10.1016/j.tws.2023.110650

[24] S. Black, A. Tzagiollari, S. Mondal, N. Dunne, D. B. MacManus, Mechanical behaviour of gel-filled additively-manufactured lattice structures under quasi-static compressive loading, Materials Today Communications, 2023, 35, 106164, https://doi.org/10.1016/j.mtcomm.2023.106164

[25] S. Kedziora, T. Decker, E. Museyibov, Application of functionally graded shell lattice as infill in additive manufacturing, Materials, 2023, 16, 4401, doi:10.3390/ma16124401

[26] V. Tuninetti, S. Narayan, I. Ríos, B. Menacer, R. Valle, M. Al-lehaibi, M. U. Kaisan, J. Samuel, A. Oñate, G. Pincheira, A. Mertens, L. Duchêne, C. Garrido, Biomimetic lattice structures design and manufacturing for high stress, deformation, and energy absorption performance, Biomimetics, 2025, 10(7), 458, doi: 10.3390/biomimetics10070458

[27] E. Cuan-Urquizo, R. Guerra Silva, Fused filament fabrication of cellular, lattice and porous mechanical metamaterials: a review, Virtual and Physical Prototyping, 2023, 18(1), 1-42, https://doi.org/10.1080/17452759.2023.2224300

[28] N. Krajangsawasdi, L. G. Blok, I. Hamerton, M. L. Longana, Fused Deposition Modelling of Fibre Reinforced Polymer Composites: A Parametric Review, J. Compos. Sci. 2021, 5, 29, https://doi.org/10.3390/jcs5010029

[29] K. K. Agarwal, G. Agarwal, A study of mechanical properties of epoxy resin in presence of different hardeners, Conference: Technological Innovation In

Mechanical Engineering (2019) https://www.researchgate.net/publication/333748514

[30] N. Sathishkumar, B. Vincent, N. Arunkumar, K. M. Kumar, P. L. Sudharsan, Study of compressive behaviour on 3D printed ABS polymer lattice structures infilled with epoxy and polyester resins, IOP Conf. Series: Materials Science and Engineering 923 (2020) 012044, doi:10.1088/1757-899X/923/1/012044

[31] J. Maszybrocka, M. Dworak, G. Nowakowska, P. Osak, B. Łosiewicz, The Influence of the Gradient Infill of PLA Samples Produced with the FDM Technique on Their Mechanical Properties, Materials 2022, 15, 1304, https://doi.org/10.3390/ma15041304

[32] ISO 527-2:2012. Determination of Tensile Properties—Part 2: Test Conditions for Moulding and Extrusion Plastics. International Organization for Standardization, Geneva, Switzerland, 2012

[33] ISO 178:2019. Plastics—Determination of Flexural Properties. International Organization for Standardization, Geneva, Switzerland, 2019

[34] ISO 604:2002. Plastics—Determination of Compressive Properties. International Organization for Standardization, Geneva, Switzerland, 2002

[35] S. Tandon, R. Kacker, K. G. Sudhakar, Quantitative strength analysis for 3D-printed specimens in a Tri-Hexagon pattern, Proc IMechE Part C: J Mechanical Engineering Science 2021, Vol. 235(24) 7685-7698, DOI: 10.1177/09544062211021120